Nanoscale Ferroelectric and Piezoelectric Properties of Sb_2S_3 Nanowire Arrays

Justin Varghese[*,†,‖], *Sven Barth*[*,‖,‡], *Lynette Keeney*[†], *Roger W. Whatmore*[†,*] *and Justin D. Holmes*[*,†,‖,*]

[*]Materials Chemistry and Analysis Group, Department of Chemistry, University College Cork, Cork, Ireland.

[†]Tyndall National Institute, University College Cork, Lee Maltings, Dyke Parade, Cork, Ireland.

[‖]Centre for Research on Adaptive Nanostructures and Nanodevices (CRANN), Trinity College Dublin, Dublin 2, Ireland.

[‡]Institute for Materials Chemistry, Vienna University of Technology, 1060 Vienna, Austria.

* roger.whatmore@tyndall.ie and j.holmes@ucc.ie

RECEIVED DATE (to be automatically inserted after your manuscript is accepted if required according to the journal that you are submitting your paper to)

TITLE RUNNING HEAD Ferroelectric Sb_2S_3 nanowire arrays

CORRESPONDING AUTHOR FOOTNOTE Roger W. Whatmore, Email: roger.whatmore@tyndall.ie or Justin D. Holmes, E-mail: j.holmes@ucc.ie, Tel: +353 (0)21 4903608; Fax: +353 (0)21 4274097.

ABSTRACT

We report the first observation of piezoelectricity and ferroelectricity in individual Sb_2S_3 nanowires embedded in anodic alumina oxide templates. Switching spectroscopy-piezoresponse force microscopy (SS-PFM) measurements demonstrate that individual, *c*-axis-oriented Sb_2S_3 nanowires exhibit ferroelectric as well as piezoelectric switching behavior. Sb_2S_3 nanowires with nominal diameters of 200 and 100 nm showed $d_{33(eff)}$ values around 2 pm V^{-1}, while the piezo coefficient obtained for 50 nm diameter nanowires was relatively low at around 0.8 pm V^{-1}. A spontaneous polarization (P_s), of approximately 1.8 μC cm^{-2}, was observed in the 200 and 100 nm Sb_2S_3 nanowires, which is a 100 % enhancement when compared to bulk Sb_2S_3 and is probably due to the defect-free, single-crystalline nature of the nanowires synthesized. 180° ferroelectric mono-domains were observed in Sb_2S_3 nanowires due to uniform polarization alignment along the polar *c*-axis.

KEYWORDS: Nanowires, Sb_2S_3, Template, Piezoelectric, Ferroelectric, PFM.

BRIEFS: Ferroelectric Sb_2S_3 nanowire arrays

Diminishing dimensions in ferroelectric/piezoelectric materials reveal pronounced size dependent effects,[1-3] which are of great interest in both fundamental and applied research.[2,4] As the dimensions of a ferroelectric material shrink, changes in remnant polarization, dielectric permittivity, phase transition temperature, coercive field, and domain structure occur.[3-6] Recent advances in nano-ferroelectrics, especially their synthesis and characterization, have provided an impetus for the development of novel nanoscale ferroelectric[7] and piezoelectric device structures.[8] Ferroelectrics can store information by switching polarization of individual domains. Shrinking the size of the ferroelectric domains to the nanoscale could be useful for high density data storage.[9] The smallest isolated ferroelectric domains of ~ 2 nm size have been experimentally demonstrated using lithium tantalate single crystals with an estimated ferroelectric storage capacity of ~ 160 Terabyte in^{-2}.[10] Additionally, piezoelectric nanowires have been used in energy harvesting devices due to their mechanical robustness and high sensitivity to mechanical stimuli, *e.g.* zinc oxide (ZnO) nano-generators.[11,12] Apart from the applications side, there is significant scientific benefit to exploring fundamental and theoretical aspects of size-dependent properties of various nanoscale ferroelectric and piezoelectric materials.[1,2,5,13] Among ferroelectric nanostructures, one-dimensional structures such as nanowires, nanorods and nanotubes have been widely explored from both theoretical and application viewpoints.[1-3,14] Studies on the size-dependant properties in ferroelectrics have revealed that one-dimensional nanostructures can enhance or reduce the ferroelectric and piezoelectric response depending on their size and morphology, defects, crystal structure, ferroelectric domain structure *etc*.[2,3] A doubling of the spontaneous polarization was observed in Rochelle salt nanowires, with a diameter of 30 nm, compared to the bulk due to the uniform polarization orientation and single crystalline nature of the wires. Precise chemical composition, high crystallinity and uniform geometry are required for defined ferroelectric material properties at the nanoscale.[15]

Most of the interest in nanoscale ferroelectric research has focused on perovskite-based complex oxide

materials, while non-oxide based ferroelectric materials so far have been left unexplored.[16] Theoretical simulations show that the highly anisotropic ion polarizability in sulfides can generate ferroelectric phase transitions.[17] Calculations of the polarizability constants of Sb_2S_3 show that a stibnite-type (Sb_2S_3) structure is favorable for a ferroelectric phase transition.[17] Grigas *et al.* reported that Sb_2S_3 exhibits two ferroelectric phase transitions at 292 K and 420 K.[18] The structural change from D_{2h}^{16} to C_{2v}^{9} accounts for the phase transition at 420 K, but no structural change has been reported for the 292 K transition.[18,19] Sb_2S_3 is polar at room temperature and the structure contains infinite ribbons of $(Sb_4S_6)_n$ along the *c*-axis.[19] These $(Sb_4S_6)_n$ chains are linked by a '2_1' screw axis in such a way that the antimony in one chain is connected to the sulfur in the neighboring chain.[19,20] The origin of ferroelectricity in Sb_2S_3 is associated with the small dipole changes in the coordination sphere of Sb and S atoms along the *c*-axis in the $(Sb_4S_6)_n$ chains.[17,18,21] Due to the anisotropy of the $(Sb_4S_6)_n$ chains along the *c*-axis the observed polarization is largely anisotropic, which was demonstrated by Grigas and Karpus.[17,21,22] This anisotropy in dielectric behaviour in Sb_2S_3 sparked our interest to explore the ferroelectric and piezoelectric behavior of this material at the nanoscale, as potentially *c*-axis-oriented single crystalline Sb_2S_3 nanowires could show highly anisotropic ferroelectric and even piezoelectric properties. Although the synthesis and characterisation of various types of Sb_2S_3 nanostructures have been the basis of numerous studies,[23-25] no data have been reported on their nanoscale ferroelectric or piezoelectric behavior.

We report the fabrication of arrays of Sb_2S_3 nanowires within cylindrical pores of anodic alumina (AAO) templates (Sb_2S_3-AAO), by a solvent-less technique utilizing the single-source precursor (SSP) antimony (III) tris(diethyldithiocarbamate), $Sb(S_2CNEt_2)_3$ (see Supporting Information, section S1.). The template-based approach to synthesize Sb_2S_3 nanowire arrays has the advantage of good control over the morphology and geometry of the nanowires and also is an effective option for making

vertically aligned arrays of nanowires.[26] In addition, the use of a template eliminates the agglomeration of the nanowires in an ordered array, which makes it possible to address the functionality of individual nanowires on a one-to-one basis. AAO membranes with nominal pore diameters ~200, 100 and 50 nm, were used as templates to prepare arrays of Sb_2S_3 nanowires. Figure 1(a) shows a top-down view of Sb_2S_3 nanowires with a nominal diameter of 200 nm within the pores of an AAO template after polishing. Cross sections of the samples, thickness 10 μm, were used to analyze the extent of Sb_2S_3 filling of the channels within the membranes (Figure 1(b)). Sb_2S_3 nanostructures showed radial dimensions in accordance with the nominal channel width of the AAO templates used, *i.e.* mean diameters of 50, 100, 200 nm. The Lorentzian diameter distribution of the Sb_2S_3 nanowires (see Supporting Information, figure S2.) formed inside the AAO membranes showed diameter distributions of 199 ± 16 nm, 93 ± 9 nm, and 51 ± 6 nm for 200, 100 and 50 nm diameter membranes respectively. The nanowire diameter distributions were calculated from plan-view scanning electron micrograph (SEM) images of polished Sb_2S_3-AAO samples. The extent of pore filling by Sb_2S_3 inside the AAO channels were ~ 80 % across a 50 μm × 50 μm area and length wise ~90 % along 10 μm long pores, irrespective of the pore diameter, with densities of 1.0×10^9, 7.6×10^8, and 4.0×10^8 nanowires per cm^2 for 50, 100 and 200 nm Sb_2S_3-AAO samples respectively. The phase purity of the material was investigated by X-ray diffraction (XRD) analysis and performed on polished Sb_2S_3-AAO samples. The XRD pattern shown in figure 1(c) can be indexed to an orthorhombic Sb_2S_3 phase (JCPDS file No: 42-1393), displaying a high intensity reflection at 47.5° originating from the (002) planes; an indication of the *c*-axis-oriented growth of the Sb_2S_3 nanowires within the templates. Energy dispersive X-ray (EDX) analysis confirmed the chemical composition of the Sb_2S_3 nanowires (figure 1(d)) to be Sb 40.5 atomic % and S 59.5 %, which is close to the theoretical values (Sb 40 %, S 60 %) for Sb_2S_3. Figure 1(e) show transmission electron micrograph (TEM) images of an Sb_2S_3 nanowire, liberated from an AAO template, revealing the single crystalline nature of the nanowire with a growth direction along the *c*-axis (<001> axis). The reflection planes parallel to the Sb_2S_3 nanowire axis shows a lattice fringe spacing of

0.801 nm, which corresponds to the inter planar (*d*) spacing between the (110) planes of orthorhombic Sb_2S_3.[19] A small area electron diffraction (SAED) pattern obtained from a Sb_2S_3 nanowire shown in figure 1(e) in the [110] zone-axis confirming the *c*-axis-oriented growth of Sb_2S_3 nanowire corresponding to orthorhombic Sb_2S_3.[19]

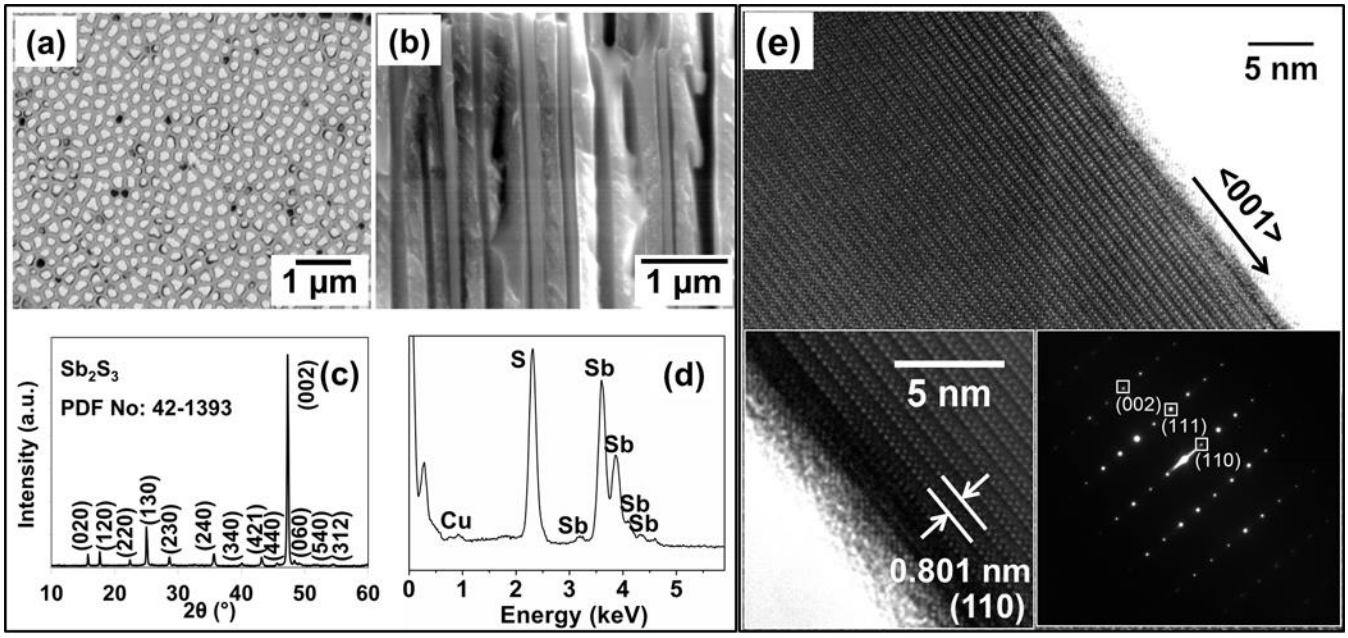

Figure 1. (a) A plan view SEM image of a surface polished 200 nm Sb_2S_3-AAO sample, (b) cross-sectional view of a 200 nm Sb_2S_3-AAO, (c) XRD pattern of a polished Sb_2S_3-AAO sample, indexed to the orthorhombic Sb_2S_3 (JCPDS file No: 42-1393) structure, (d) EDX spectrum of an isolated 200 nm Sb_2S_3 nanowire after removal from an AAO template and (e) HRTEM image of an Sb_2S_3 nanowire liberated from an AAO template with a nominal pore diameter of 200 nm (inset: magnified TEM image and SAED pattern of the single crystalline Sb_2S_3 shown in (e) nanowire with a <001> growth direction and imaged in the [110] zone axis).

The ferroelectric and piezoelectric functionality of individual Sb_2S_3 nanowires inside the AAO membranes was demonstrated using piezo force microscopy (PFM), in contact mode, along the *c*-axis at

room temperature (see Supporting Information, section S2). In order to align the polarization of the Sb_2S_3 nanowires, an axial bias voltage of ± 44 V was applied to a 2.5 × 2.5 μm^2 surface area of the Sb_2S_3-AAO samples, between the back electrode and the conducting PFM tip in contact mode. Figure 2 illustrates the PFM height profile, the resulting piezo-response amplitude and the phase signal of Sb_2S_3-AAO samples with various mean diameters (magnified PFM images are provided in Supporting Information, figure S4.). The amplitude signal is a direct measure of the piezoelectric response of the material. The Sb_2S_3 nanowires, irrespective of the diameter, showed positive domains (white contrast) in the amplitude signal which is a clear indication of a piezo response in the nanowires due to out-of plane polarization. Sb_2S_3 nanowires inside AAO pores with nominal diameters 200, 100 and 50 nm showed a maximum vibration amplitude of ~500, ~350 and ~100 pm respectively. The piezo amplitude response observed in the Sb_2S_3 nanowires is the contribution from *c*-axis oriented mono-domains within the probing volume underneath the tip. Some of the Sb_2S_3 nanowires regardless of their diameter, showed no piezo response, which may be due to the poor accessibility of the PFM tip to these nanowire inside the AAO channels. 200, 100 and 50 nm Sb_2S_3 nanowires showed out-of plane polarization (vertical piezo amplitude response) meaning that the polarization is parallel and aligned with the applied electric field and causes a local expansion of the nanowires.[27] The phase images of Sb_2S_3 nanowires with various diameters (figure 2) clearly show a high percentage of uniformly polarized nanowires with single ferroelectric domains; the size of these domains limited by the diameter of the nanowires. The reason for the existence of mono-domains can be attributed to the single crystalline (<001> oriented) low defect nature of Sb_2S_3 nanowires, as is evident from the high resolution TEM images. As the *c*-axis (<001> direction) is the polar axis of the Sb_2S_3 nanowires, a high percentage of up- and downward polarized domains were formed along the *c*-axis of the Sb_2S_3 nanowires.[28-30] Detailed examination of PFM phase images from Sb_2S_3-AAO samples (see Supporting Information, figure S5.) revealed the presence of multi-domain ferroelectric structures in some of the nanowires, probably due to defects created on the surface of these nanowires upon mechanical

150 polishing.[27,31]

151

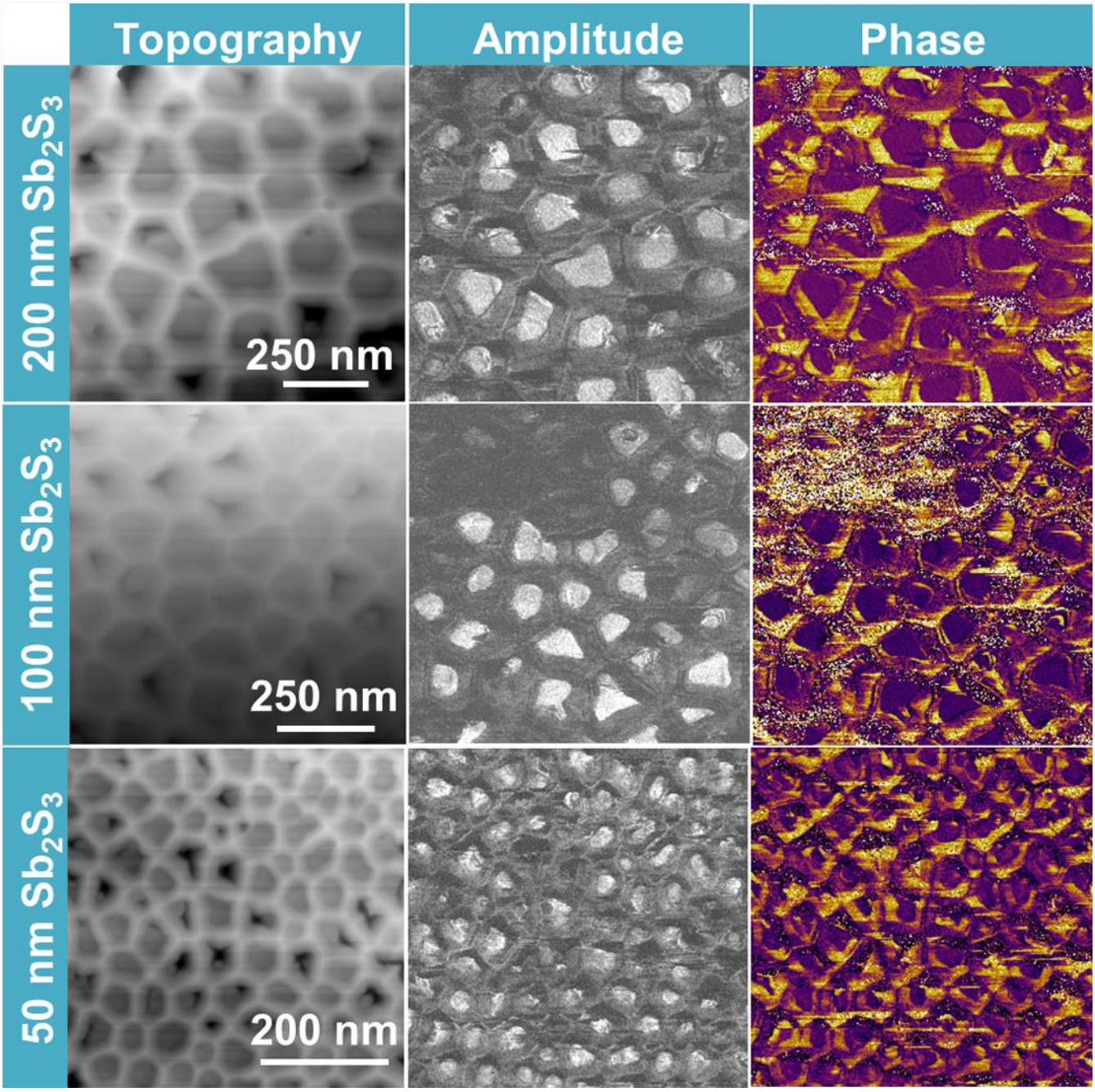

152

153 **Figure 2.** PFM images showing topography, amplitude and phase profiles of Sb_2S_3-AAO samples of

154 various diameters.

155

156 The characteristic of ferroelectric materials is the switching of the polarization by an applied electric

157 field. The spectroscopy mode of PFM (SS-PFM) is widely used to understand the switching behaviour

158 in nano-ferroelectrics.[32-34] The piezoelectric hysteresis loops were obtained by positioning the
159 conductive PFM tip in the center of any chosen Sb_2S_3 nanowire within the AAO pores and an AC
160 voltage of 3.3 V was applied, whilst a biased DC voltage of ± 44 V was applied across the nanowire
161 between the PFM tip and the back electrode (gold). Applying a small AC voltage through the PFM tip
162 to an individual Sb_2S_3 nanowire inside an AAO pore leads to local structural deformation, due to a
163 converse piezoelectric effect and the resulting strain from the nanowire surface is detected by the PFM
164 tip to generate a piezoelectric hysteresis loop. The amplitude of the detected piezoelectric vibration
165 from a Sb_2S_3 nanowire is a direct measure of a nanowire's piezoelectric coefficient, whereas the phase
166 of the signal relates to the polarization direction present in the nanowire. The remnant phase and piezo
167 switching hysteresis observed in the Sb_2S_3 nanowires with various diameters are shown in figures 3(a)
168 and 3(b). Figure 3(a) shows the phase-voltage hysteresis loops obtained for Sb_2S_3-AAO samples with
169 mean diameters of 200, 100 and 50 nm. The square-shaped phase hysteresis loops obtained for all of
170 the Sb_2S_3-AAO samples investigated exhibited a 180° domain reversal, which is a signature of the
171 presence of ferroelectricity in the nanowires. The180° phase reversal of the polarization during the
172 voltage sweep is an indication of switchable ferroelectricity in Sb_2S_3 nanowires. The origin of
173 ferroelectricity in Sb_2S_3 at room temperature can be explained by the polar C_{2v}^9 symmetry of the
174 orthorhombic Sb_2S_3 crystal.[19] The polarization results from a small movement of Sb and S atoms within
175 the two $(Sb_4S_6)_n$ chains along the *c*-axis, and so the associated change in polarization will be confined to
176 one direction in space.[21,22]
177
178 Sb_2S_3 nanowires also showed piezoelectric behavior. The normalized piezo-response hysteresis loops
179 obtained for Sb_2S_3-AAO samples with various mean diameters is shown in figure 3(b). 200 and 100 nm
180 Sb_2S_3-AAO samples showed well defined piezoelectric switching hysteresis, while 50 nm samples
181 showed very weak piezo switching. The surface of polished 50 nm Sb_2S_3-AAO samples were found to
182 be rougher than those of the 100 and 200 nm samples, consequently leading to a decrease in the tip-

surface contact quality and in turn affecting the acquisition of high quality PFM hysteresis loops.[27,33] However, a study by Zhang *et al.* on PZT-AAO samples also suggests the possible influence of nanowire-AAO wall interfaces on the PFM piezo-response signal.[35] The exact reason for the reduced piezoelectric coefficient and polarization in the thinnest Sb_2S_3 nanowires in this study therefore needs further investigation. A quantitative measure of the piezo response of Sb_2S_3 nanowires was made by calculating the piezoelectric coefficients from the SS-PFM piezo amplitude hysteresis data. The measured piezoelectric coefficient, which is designated as $d_{33(eff)}$ ('effective' d_{33} coefficient) represents the electromechanical response from a Sb_2S_3 nanowire inside an AAO pore in the *z* direction when an electric field is applied in the same direction and is typically calculated from the vertical PFM data.[27] 200 and 100 nm Sb_2S_3 nanowires showed $d_{33(eff)}$ values around 2 pm V^{-1}, while the piezo coefficient obtained for 50 nm nanowires was relatively low at around 0.8 pm V^{-1}. The $d_{33(eff)}$ value obtained for Sb_2S_3 nanowires is very weak compared to other common piezoelectric nanowires, such as $(PbZr_{1-x}T_x)O_3$, ZnO and $BaTiO_3$, which are in the range of 10 to 100 pm V^{-1}.[36-38] However, there is no report to-date on the quantification of a piezo response from bulk Sb_2S_3 single crystals.

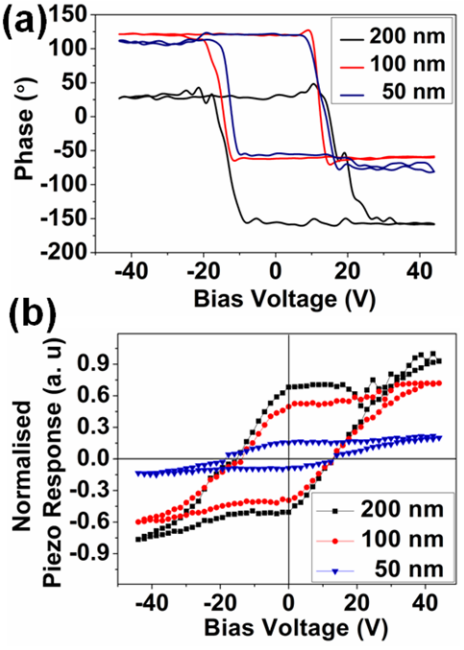

Figure 3. SS-PFM hysteresis loops acquired from an individual Sb_2S_3 nanowires inside AAO pores of various nominal diameters: (a) phase-voltage hysteresis and (b) piezo response-voltage hysteresis.

Domain switching under the application of an external field is a signature characteristic of switchable ferroelectricity. PFM is a powerful technique for probing the nucleation, growth and switching of ferroelectric domains in nanoscale ferroelectrics.[34,39,40] Figure 4 illustrates the ferroelectric domain switching properties of Sb_2S_3-AAO samples under the application of an external bias, and provides conclusive evidence for the presence of switchable ferroelectricity in Sb_2S_3 nanowires. Figures 4(a) and 4(b) represents the topography and PFM phase image before switching. The domain switching was observed in Sb_2S_3 nanowires when an applied bias of -33 V was applied, as seen by the change in color contrast of the PFM phase image (figure 4(c)). The application of an opposite bias of +33 V on the same area reversed the domain structure of the nanowires (figure 4(d)). To check the effect of the applied bias on the domain switching characteristics, an increased bias of ±44 V was applied to the nanowires (figures 4(f) and 4(g)). The uniform color contrast observed in the PFM phase image after applying a bias of -44 V (figure 4(f)) indicates complete switching to a stable opposite polarization state.

The presence of ferroelectricity in arrays of Sb_2S_3 nanowires (Gold/Sb_2S_3-AAO/Gold capacitor geometry (see Supporting Information, section S3) was also confirmed from the polarization-electric field (*P-E*) hysteresis loop as a "nanowire-bulk" measurement (figure 5). The well-defined *P-E* hysteresis loop obtained for Sb_2S_3 nanowires, irrespective of their mean diameter, is conclusive evidence for the presence of ferroelectricity and supports the data obtained from PFM analysis. The shape of the *P-E* loop shows the incomplete saturation of the hysteresis, an indication of the still growing domains. This type of unsaturation is usual in weak ferroelectric materials as much higher fields are typically required to switch the domain polarization. 200 and 100 nm Sb_2S_3 nanowires show a spontaneous polarization (P_s) of ~1.8 μC cm^{-2} and 50 nm nanowires P_s ~1 μC cm^{-2}. The spontaneous polarization observed in the Sb_2S_3 nanowires is small compared to other perovskite-based ferroelectric nanowires such as PZT nanowire.[8] During polarization switching, in perovskite ferroelectrics,

displacement of atoms causes polarity changes in the whole lattice, which results in a massive polarization, *i.e.* via a displacement mechanism.[15] In contrast, the polarization reversal in Sb_2S_3 is a result of an order-disorder transition in the $(Sb_4S_6)_n$ chains which creates only a small polar distortion of the lattice and results in a weak spontaneous polarization.[18] The same reasoning can be applied to the weak piezoelectric behavior of Sb_2S_3 nanowires. Sb_2S_3 nanowires, irrespective of their mean diameter, showed a remnant polarization (P_r) and coercive field of switching (E_c), obtained from the *P-E* loop, of approximately 1 μC cm^{-2} and 50 kV cm^{-2} respectively.

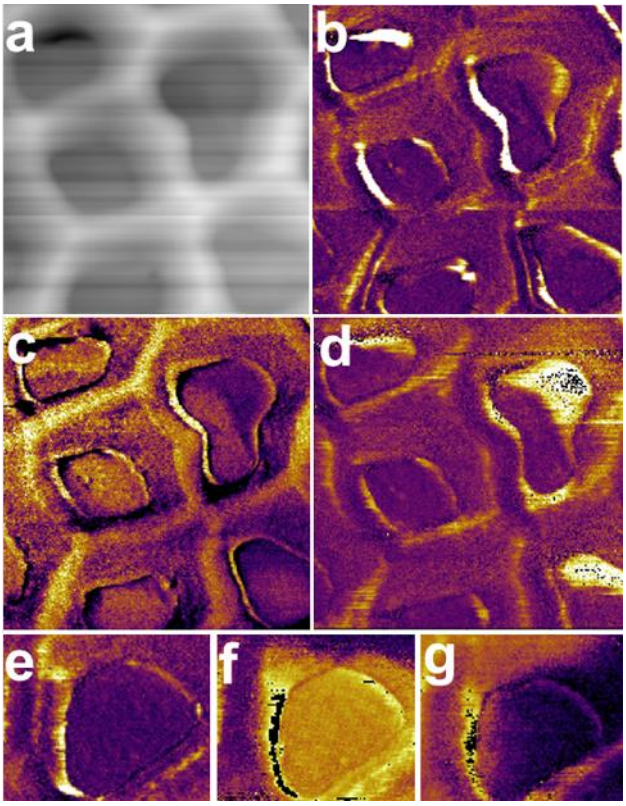

Figure 4. Ferroelectric domain switching of a selected area of Sb_2S_3-AAO sample: (a) topographic image, (b) PFM phase image before switching, (c) after switching of the area by applying –33 V and (d) after applying + 33 V. Ferroelectric domain switching of a selected Sb_2S_3 nanowire, (e) PFM phase image before switching, (f) after switching of the nanowire by applying –44 V and (g) after applying + 44 V.

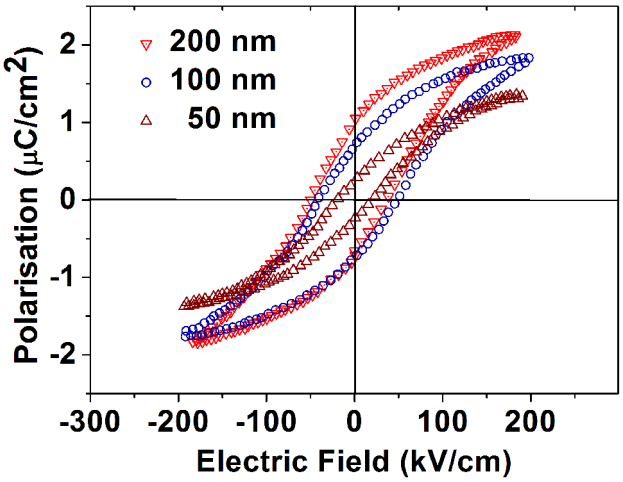

Figure 5. Polarization-electric field hysteresis loop of Sb_2S_3-AAO samples with various mean diameters.

Significantly the spontaneous polarization observed in our Sb_2S_3 nanowires showed an enhancement compared to the bulk. At room temperature bulk Sb_2S_3 shows a spontaneous polarization of ~ 1.0 μC cm^{-2}, which means the polarization was almost doubled in the nanowires.[19] A similar enhancement was observed in Rochelle salt single crystalline nanowires templated within the pores of AAO membranes[29], where the enhancement was attributed to the presence of multiple nano-domains with uniform orientation along the direction of the applied electric field. Morozovska *et al.*[2], in their study on ferroelectricity enhancement in confined nanorods, proposed that the ferroelectric property enhancement in nanowires and nanorods was due to the long-range interactions along the polar axis.[2,30] Also a uniform crystallographic orientation will enhance the uniform alignment of ferroelectric nano-domains.[29] In Sb_2S_3 nanowires, the formation of 180° domains with polarization directions pointing along +*z* and –*z* directions leads to a decrease in the depolarizing field, which enhances the spontaneous polarization especially in one dimensional ferroelectrics.[41] The single crystalline nature of Sb_2S_3 nanowires (*c*-axis oriented) and their long range order inside AAO templates can also align dipoles

261 preferentially along the nanowire polar *c*-axis.

262

263 In summary, the presence of ferroelectricity and piezoelectricity in Sb_2S_3 nanowires was demonstrated
264 for the first time using piezoresponse force microscopy. Sb_2S_3 nanowires showed polarization and
265 amplitude switching hysteresis, which is a signature of the ferroelectric and piezoelectric behavior.
266 High density arrays of Sb_2S_3 nanowires showed mostly 180° single domain polarization owing to the c-
267 axis-oriented single crystalline nature of the nanowires. Sb_2S_3 nanowires showed an enhanced
268 spontaneous polarization compared to bulk, due to the uniform orientation of domains along the
269 direction of an applied electric field.

270

271 Supporting Information

272 Synthesis of single source precursor, experimental method, diameter distribution of nanowires and
273 supporting data on PFM analysis. This material is available free of charge via the Internet at
274 http://pubs.acs.org.

275

276 ACKNOWLEDGMENT. This work was supported by Science Foundation Ireland (SFI) under the
277 FORME Strategic Research Cluster Award (Project 07/SRC/I1172). This research was also enabled by
278 the Higher Education Authority Program for Research in Third Level Institutions (2007-2011) via the
279 INSPIRE programme. We are thankful to Mr. Nitin Deepak for help on PFM imaging and processing.

280

281

References

(1) Scott, J. F. *Ferroelectrics* **2005**, *316*, 13

(2) Morozovska, A. N.; Eliseev, E. A.; Glinchuk, M. D. *Phys Rev B* **2006**, *73*.

(3) Morozovska, A. N.; Glinchuk, M. D.; Eliseev, E. A. *Phase Transitions* **2007**, *80*, 71.

(4) Saad, M. M.; Baxter, P.; McAneney, J.; Lookman, A.; Sinnamon, L. J.; Evans, P.; Schilling, A.; Adams, T.; Zhu, X. H.; Pollard, R. J.; Bowman, R. M.; Gregg, J. M.; Jung, D. J.; Morrison, F. D.; Scott, J. F. *Ieee Transactions on Ultrasonics Ferroelectrics and Frequency Control* **2006**, *53*, 2208.

(5) Scott, J. F.; Morrison, F. D.; Miyake, M.; Zubko, P. *Ferroelectrics* **2006**, *336*, 237

(6) Naumov, I. I.; Fu, H. *Phys. Rev. Lett.* **2005**, *95*, 247602.

(7) Evans, P. R.; Zhu, X.; Baxter, P.; McMillen, M.; McPhillips, J.; Morrison, F. D.; Scott, J. F.; Pollard, R. J.; Bowman, R. M.; Gregg, J. M. *Nano Lett.* **2007**, *7*, 1134.

(8) Xu, S.; Hansen, B. J.; Wang, Z. L. *Nat Commun* **2010**, *1*, 93.

(9) Lee, W.; Han, H.; Lotnyk, A.; Schubert, M. A.; Senz, S.; Alexe, M.; Hesse, D.; Baik, S.; Gosele, U. *Nat Nano* **2008**, *3*, 402.

(10) Tanaka, K. Y., K.; Tomoya, U.; Yasuhiro, D.; Nozomi, O.; Ryusuke, H.; Yoshiomi, H.; Yasuo, C. *Jpn J Appl Phys* **2008**, *47*.

(11) Wang, Z. L.; Song, J. *Science* **2006**, *312*, 242.

(12) Barth, S.; Hernandez-Ramirez, F.; Holmes, J. D.; Romano-Rodriguez, A. *Prog. Mater Sci.* **2010**, *55*, 563.

(13) Rodriguez, B. J.; Gao, X. S.; Liu, L. F.; Lee, W.; Naumov, I. I.; Bratkovsky, A. M.; Hesse, D.; Alexe, M. *Nano Lett.* **2009**, *9*, 1127.

(14) Kim, J.; Yang, S. A.; Choi, Y. C.; Han, J. K.; Jeong, K. O.; Yun, Y. J.; Kim, D. J.; Yang, S. M.; Yoon, D.; Cheong, H.; Chang, K. S.; Noh, T. W.; Bu, S. D. *Nano Lett.* **2008**, *8*, 1813.

(15) Haertling, G. H. *J. Am. Ceram. Soc.* **1999**, *82*, 797.

(16) Gruverman, A.; Kholkin, A. *Rep. Prog. Phys.* **2006**, *69*, 2443.

(17) Grigas, J. *Microwave dielectric spectroscopy of ferroelectrics and related materials*; Gordon and Breach Publishers: Amsterdam B.V., 1996; Vol. 9.

(18) Grigas, J. *Ferroelectrics* **1978**, *20*, 173

(19) O. Madelung, U. R., M. Schulz. In *Landolt-Börnstein - Group III Condensed Matter*; Springer-Verlag: 1998; Vol. 41C.

(20) Arun, P.; Vedeshwar, A. G. *J Mater Sci* **1996**, *31*, 6507.

(21) Grigas, J.; Talik, E.; Lazauskas, V. *Phase Transitions: A Multinational Journal* **2002**, *75*, 323

(22) Petzelt, J.; Grigas, J. *Ferroelectrics* **1973**, *5*, 59

(23) Bin Yang, R.; Bachmann, J.; Reiche, M.; Gerlach, J. W.; Gosele, U.; Nielsch, K. *Chem. Mater.* **2009**, *21*, 2586.

(24) Bin Yang, R.; Bachmann, J.; Pippel, E.; Berger, A.; Woltersdorf, J.; Gosele, U.; Nielsch, K. *Adv. Mater.* **2009**, *21*, 3170.

(25) Bao, H. F.; Cui, X. Q.; Li, C. M.; Song, Q. L.; Lu, Z. S.; Guo, J. *J Phys Chem C* **2007**, *111*, 17131.

(26) Routkevitch, D.; Tager, A. A.; Haruyama, J.; Almawlawi, D.; Moskovits, M.; Xu, J. M. *Ieee Transactions on Electron Devices* **1996**, *43*, 1646.

(27) Balke, N.; Bdikin, I.; Kalinin, S. V.; Kholkin, A. L. *J. Am. Ceram. Soc.* **2009**, *92*, 1629.

(28) Wang, Z.; Hu, J.; Yu, M.-F. *Appl. Phys. Lett.* **2006**, *89*, 263119.

(29) Yadlovker, D.; Berger, S. *Phys Rev B* **2005**, *71*, 184112.

(30) Morozovska, A. N.; Eliseev, E. A.; Glinchuk, M. D. *Physica B: Condensed Matter* **2007**, *387*, 358.

(31) Kalinin, S. V.; et al. *Rep. Prog. Phys.* **2010**, *73*, 056502.

(32) Jesse, S.; Baddorf, A. P.; Kalinin, S. V. *Appl. Phys. Lett.* **2006**, *88*, 062908.

(33) Jesse, S.; Lee, H. N.; Kalinin, S. V. *Rev. Sci. Instrum.* **2006**, *77*, 073702.
(34) Rodriguez, B. J.; Jesse, S.; Alexe, M.; Kalinin, S. V. *Adv. Mater.* **2008**, *20*, 109.
(35) Zhang, X. Y.; Zhao, X.; Lai, C. W.; Wang, J.; Tang, X. G.; Dai, J. Y. *Appl. Phys. Lett.* **2004**, *85*, 4190.
(36) Fujisawa, H.; Kuri, R.; Shimizu, M.; Kotaka, Y.; Honda, K. *Appl. Phys. Express* **2009**, *2*.
(37) Wang, Z.; Suryavanshi, A. P.; Yu, M.-F. *Appl. Phys. Lett.* **2006**, *89*, 082903.
(38) Zhao, M.-H.; Wang, Z.-L.; Mao, S. X. *Nano Lett.* **2004**, *4*, 587.
(39) Morozovska, A. N.; Svechnikov, S. V.; Eliseev, E. A.; Jesse, S.; Rodriguez, B. J.; Kalinin, S. V. *J. Appl. Phys.* **2007**, *102*, 114108.
(40) Morozovska, A. N.; Eliseev, E. A.; Kalinin, S. V. *Appl. Phys. Lett.* **2006**, *89*, 192901.
(41) Naumov, I. I.; Bellaiche, L.; Fu, H. *Nature* **2004**, *432*, 737.

344 **Table of Contents Graphic**

345